

# Prediction of the Functional Performance of Machined Components Based on Surface Topography: State of the Art

Wit Grzesik

(Submitted January 29, 2016; in revised form May 25, 2016; published online August 31, 2016)

This survey overviews the functional performance of manufactured components produced by typical finishing machining operations in terms of their topographical characteristics. Surface topographies were characterized using both profile (2D) and 3D (areal) surface roughness parameters. The prediction of typical functional properties such as fatigue, friction, wear, bonding and corrosion is discussed based on appropriate surface roughness parameters. Some examples of real 3D surface topographies produced with desired functional characteristics are provided. This survey highlights technological possibilities of producing surfaces with enhanced functional properties by machining processes.

**Keywords** functional properties, machining processes, surface roughness, surface texture

## 1. Introduction

The prediction of the functional properties of machined parts belongs to the fundamental challenges of manufacturing engineering. In general, it is based on the measurements of surface finish generated in cutting, abrasive and burnishing operations. In practice, functional properties of machined surfaces are correlated with 2D and 3D surface roughness, waviness and surface texture. It should be noted that engineering knowledge required with for the prediction of functional properties is not completed apart from the advanced surface metrology techniques (Ref 1, 2). Typically, the design of machine parts is based on the dimensional and form tolerances and fragmentally on the surface roughness parameters (predominantly roughness average Ra).

On the other hand, the functional performance is strongly related to the surface finish including surface texture and mechanical properties of the surface layer. According to the present knowledge, this relationship concerns such important functional properties as fatigue life, wear resistance, corrosion resistance, joint stiffness, lubrication and sealing abilities, etc. (Ref 3).

At present, design and manufacturing engineers are equipped with many engineering tools such as surface characterization and visualization using 2D/3D surface roughness parameters specified in ISO 25178 and ISO 16610 standards, VR software and FEM simulations. Recently, it has been proposed (Ref 4) to consider all problems related to manufacturing and exploitation of machined surfaces in a new discipline termed *Areology*, (Greek word *areo* means surface) which extends the range of existing discipline *Surface Engineering*. In

general, three groups of exploitation properties (mechanical, tribological and corrosion) are distinguished as shown in Fig. 1.

According to Whitehouse (Ref 5), it is not possible now to predict functional performance accurately based on measured surface parameters but to identify various functional regimes based on functional maps as shown in Fig. 2. As a result, functional boundaries are matched by the boundaries determined by different roughness parameters. Moreover, it is possible to consider types of surface roughness parameters rather than specific parameters. For instance, boundaries for contact and tribological interactions are distinguished by the behavior of non-dimensional parameters, namely “normal gap” and “relative movement.”

In this paper, some important functional properties including fatigue strength and fretting, sliding friction, abrasive wear resistance, adhesion and bonding and corrosion resistance are characterized in terms of 2D and 3D surface roughness parameters including both 12 S-parameters and 13 V-parameters specified in ISO 25178-2 (2012) standard (Ref 6, 7).

The importance of 3D parameters which characterize surface topography over 2D surface finish parameters is that the surface functionality depends strongly on machined lays which, in turn, influence the directionality (anisotropy) of the surface texture. The survey provides the possible relationships between various functional performance categories and five finish and topography classes.

## 2. Fatigue Strength and Fretting Wear

The influence of surface roughness (surface integrity of a greater significance) is one of the greatest and oldest concern for design components subjected to cyclical loads (Ref 4, 8). In general, low surface roughness causes better fatigue performance, but for values of the Ra parameter between 2.5 and 5  $\mu\text{m}$  residual stresses along with strain-hardening effect and material microstructure became a better indicator in relation of fatigue life. In particular, cold deformation processes such as roller burnishing and shot peening induced comprehensive

Wit Grzesik, Opole University of Technology, Str. Mikolajczyka 5, 45-271 Opole, Poland. Contact e-mail: w.grzesik@po.opole.pl.

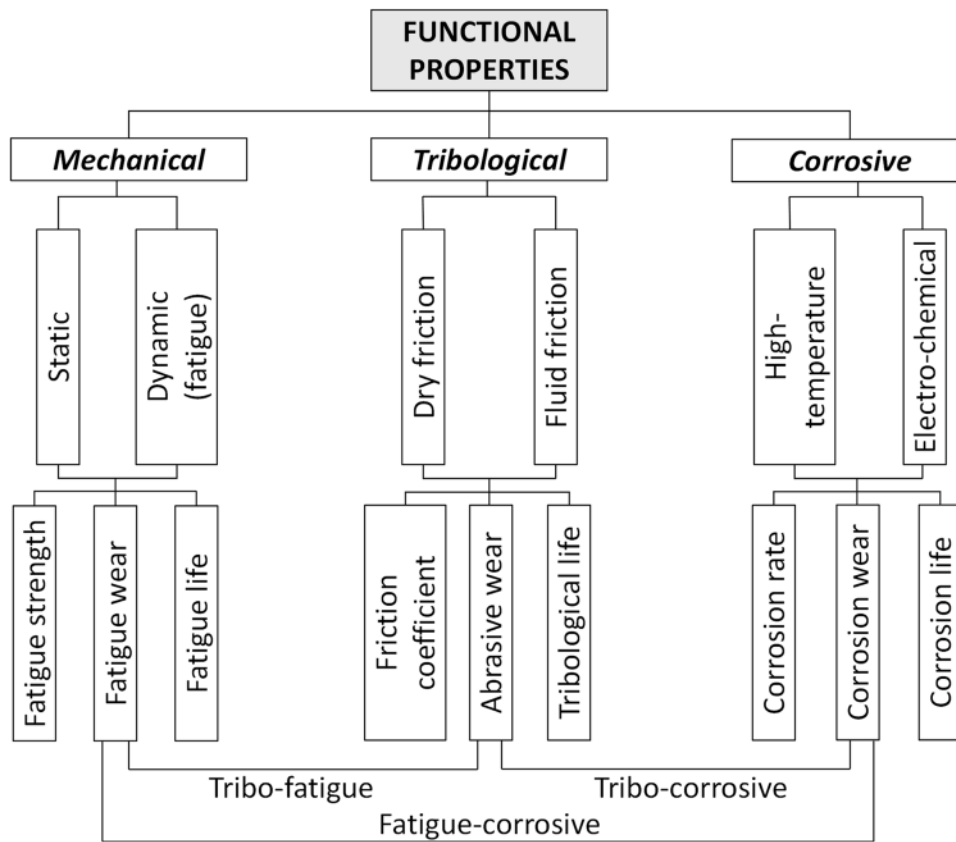


Fig. 1 Three groups of functional properties after Ref 4

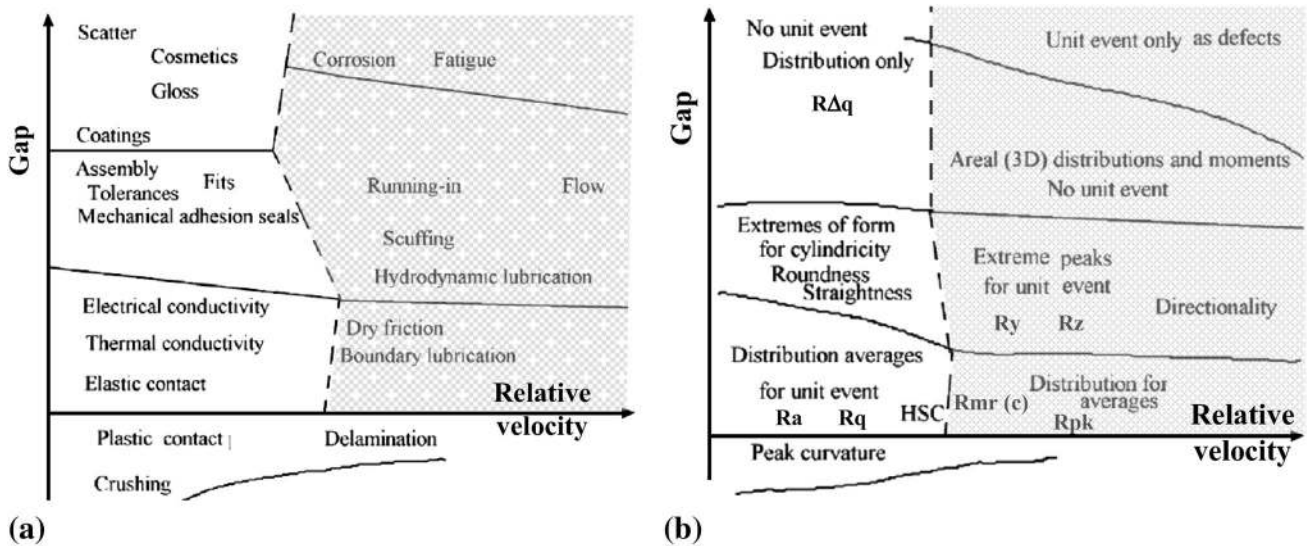


Fig. 2 Function (a) and surface parameter (b) maps after Ref 5 with modifications

residual stresses and enhanced fatigue performance. However, in the absence of residual stresses, the surface roughness  $R_a > 0.1 \mu\text{m}$  characteristic for polished or micro-finished surfaces strongly influences fatigue performance (Ref 8). When the working temperature exceeds  $400^\circ\text{C}$ , the influence of both residual stresses and surface roughness is distinctly reduced due to stress relaxation effects.

It should be noted that the testing of fatigue performance in terms of the surface topography demands employing stress-free

specimens. This effect causes that the predicted fatigue strength changes typically about 20% for surfaces with a comparable  $R_a$  value. The influence of the  $R_a$  and  $R_t$  roughness parameters on the fatigue strength of AISI 4140 (40Cr6) steel specimens is presented in Fig. 3. It should be noted that distinct variations of the measured values of  $R_a$  and  $R_t$  parameters were determined for all machined surfaces.

It can be seen in Fig. 3 that the ground surface (FG) exhibits lower fatigue strength than finish milled surface (FM) due to

unsuitable surface lays resulting in deeper microgrooves within the surface profile, which decreases fatigue strength. The positive effect of polishing (PL) in relation to finish grinding (FG) is more visible due to the smoothing effect of the surface irregularities.

It is frequently noted in literature that the maximum height roughness parameters  $R_t$  and  $R_z$  correlate better with fatigue strength than the most popular  $R_a$  parameter (see for instance the differences between the values of  $R_a$  parameter for rough and finish milled surfaces in Fig. 3).

However, as suggested in Fig. 4, the influence of the total roughness height  $R_t$  should be considered along with kurtosis  $R_{ku}$  because not only microgrooves, but also material distribution at the profile height is decisive for the stress concentration limiting the fatigue. Because machined surfaces are, in general, non-Gaussian ( $R_{sk} \neq 0$  and  $R_{ku} \neq 3$ ), both the  $R_a(R_t)$  parameter and kurtosis should be taken into account in predicting fatigue performance (Ref 7, 8).

Apart from the 2D amplitude and material distribution parameters also 3D surface spatial parameters such as the texture direction  $Std$ , the autocorrelation length  $Sal$ , the functional parameters such as the core fluid retention index  $Sci$  and the valley fluid retention index  $Svi$ , and hybrid parameters such as the arithmetic mean summit curvature  $Ssc$  should be included in correlating surface characteristics with fatigue performance of dynamically loaded parts (Ref 7).

Initial topography of contacting bodies also influences the intensity of surface degradation caused by abrasive-fatigue mode of wear term fretting, which occurs at micro-contacts of roller bearing rings and balls (Ref 4). Material losses are caused by high cyclic loads typical for fatigue. Figure 5 shows 3D morphology of fretting scar developed during a fretting test for Ti-6Al-4V titanium alloy and the AISI 52100 ball. Fretting tester with electrodynamic shaker working under 15 Hz sinusoidal displacements and the ball displacement of  $\delta = 200 \mu\text{m}$  was used.

It was observed (Ref 4) that the initial surface roughness of  $R_a = 0.25\text{--}1.5 \mu\text{m}$  influences both friction coefficient and wear volume (equivalent to the wear activation energy) and for this reason the value of  $R_a$  roughness parameter should be considered at the design stage of parts subjected to fretting wear mode (Ref 4, 9).

### 3. Sliding Friction

Tribological properties of tribo-pairs are assessed quantitatively using the friction coefficient, wear margin and tribological life (tribological margin) (Ref 4).

Friction is a very important engineering problem because about 30% of world energy consumption is used to overcome

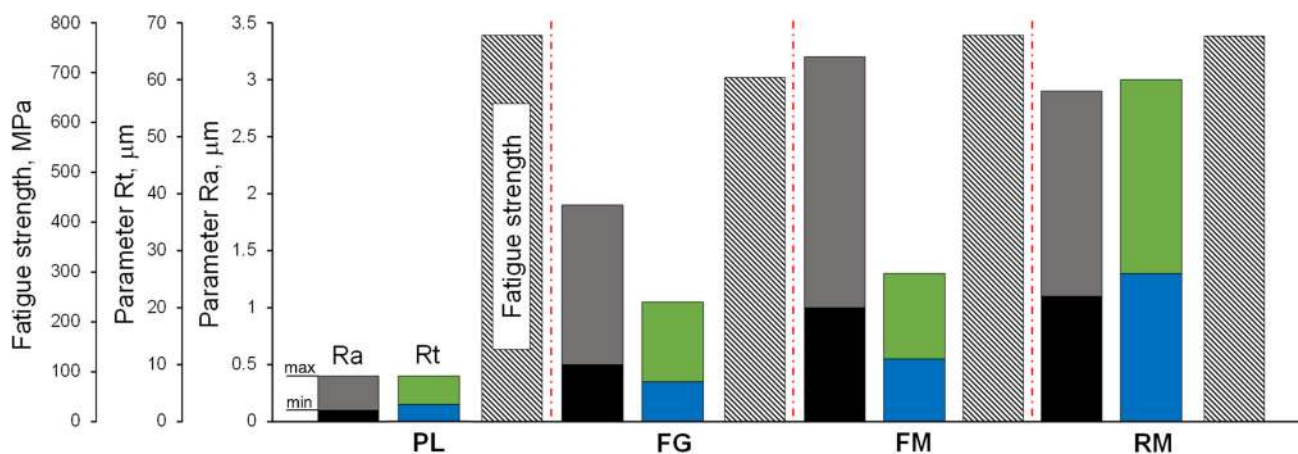


Fig. 3 Relationships between fatigue strength and amplitude roughness parameters for various machined surfaces after Ref 8: PL-polished, FG-finish ground, RM-rough milled, FM-finish milled

Function	Surface parameters				
	Height	Amplitude and shape	Hybrid and curvature	Length and peak space	Lays and texture
<b>Fatigue</b>	● ●	●	○	○	● ●
Typical 2D parameters	$R_a, R_q, R_t$	$R_{sk}, R_{ku}, R_{mr}(c)$	$R_{\Delta a}, R_{\Delta q}, \text{peak curvature}$	$R_{\lambda a}, R_{\lambda q}, P_c, \text{correlation length}$	none
Typical 3D parameters	$S_a, S_q$	$S_{sk}, S_{ku}, S_{sc}$	$S_{\Delta a}, S_{sc}$	$S_{al}, S_{dr}$	$S_{td}, S_{vi}$

Fig. 4 Effect of surface finish and topography on the fatigue strength after Ref 3 with modifications. Key: double filled circle: much evidence, single filled circle: some evidence, open circle: little evidence (see also Fig. 4, 9, 11)

excessive friction in tribo-pairs of machines and devices. In order to increase the tribological life of different tribo-pairs such as bearings, gears, cylinder-piston rings, etc., the friction coefficient should be reduced as much as possible. The 2D and 3D surface roughness parameters which influence frictional behavior are specified in Fig. 6.

In the case study presented, four topographies of machined surfaces produced by grinding (GR), honing (HN), hard turning (HT) and isotropic finishing (IF), shown in Fig. 7, generated on machine parts made of an AISI 52100 bearing steel, were characterized and compared in terms of representative 3D roughness parameters, plasticity index  $\psi$  and the value of mean friction coefficient. Friction tests were performed using a ball-on-flat tribometer and a bearing ball of about 60 HRC hardness.

The relevant values of appropriate roughness parameters are specified in Fig. 8. It should be noted in Fig. 8 that the ground surface is characterized by the highest density of summits ( $Sds \approx 5800 \text{ mm}^{-2}$ ), but the isotropic finished surface is depicted by the lowest mean slope of  $S\Delta q \approx 0.08$ .

Figure 9 shows the maximum and minimum values of kinetic friction coefficient ( $\mu_k$ ) that were determined for ground and isotropic finished surfaces, respectively. According to roughness data presented in Fig. 8, the increase in the value of

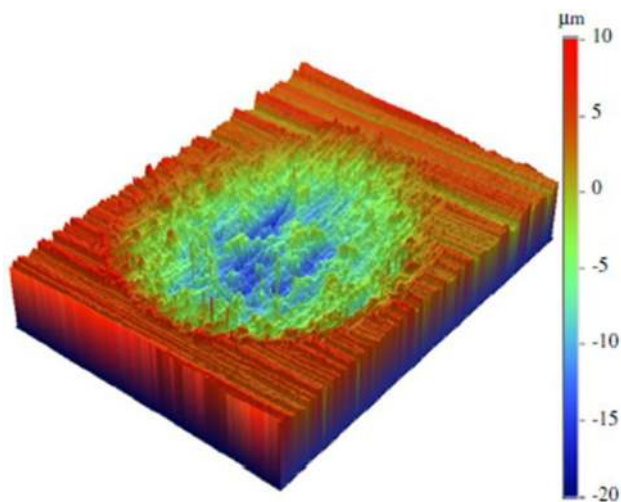


Fig. 5 Isometric view of fretting wear scars for Ti-6Al-4V alloy after Ref 9

friction coefficient for ground surfaces is about 40%. Surfaces produced by honing and hard turning are comparable in terms of their tribological properties (for both these cases  $\mu_k \approx 0.12$ ).

It can be noted that the maximum values of  $Sq$  and  $Sds$  parameters were measured for the ground surface due to the fact that it contains the highest peaks and the largest number of summits for the surface unit. In contrast, for the isotropic finished surface the  $Sq$  parameter is about 75% lower and the number of summits is about 85% less. For these reasons, the coefficient of friction for the ground surface is about 27% higher than for a very smooth surface produced by mass finishing. In addition, the value of  $Sq$  parameter is lower for the honed surface in comparison with the hard turned surface, but it contains about 50 times more peaks due to characteristic plateau structure. This means that honed surfaces indicate stronger adhesive interaction than mechanical one (inverse trend is typical for hard turned surfaces).

The values of the autocorrelation length  $Sal$  specified in Fig. 8 suggest that surface textures produced by hard turning and isotropic finishing contain components with longer wavelengths ( $Sal = 48.5$  and  $20$  respectively).

It was documented that the minimum friction achieved by isotropic finishing corresponds well with relevant values of torque and working temperature of a roller bearing. These values are lower about 20 and 40%, respectively, in comparison with ground surfaces (Ref 11).

In the case of a strongly anisotropic ground surface, the influence of lays is also important and, as a result, the friction coefficient increases by 44.5% when the friction tests are running parallel to lays. In practice, it is performed across the lays in order to reduce friction.

In addition, Fig. 10 shows the values of plasticity index  $\Psi$ , which expresses the tendency of surface irregularities to plastic deformation versus the mean surface slope  $S\Delta q$ . The higher  $\Psi$  value the higher intensity of plastic deformation (when  $\Psi < 1$  elastic deformation occurs). According to this criterion the most stiff are isotropic finished surfaces with the minimum value of the mean surface slope  $S\Delta q = 0.081$ .

An important practical finding is that both skewness and kurtosis influence static friction coefficient. It was documented (Ref 12) that a positive skewness causes that the friction coefficient decreases and, in contrast, for a negative skewness ( $Rsk < 0$ ) friction becomes more intensive than for the Gaussian distribution ( $Rsk = 0$ ,  $Rsk = 3$ ). The reverse influence of kurtosis was observed for non-Gaussian distribution, when  $Rku > 3$ .

Function \ Surface parameters	Height	Amplitude and shape	Hybrid and curvature	Length and peak space	Lays and texture
<b>Friction</b>	● ●	● ●	● ●	● ●	● ●
Typical 2D parameters	$Ra, Rq, Rt$	$Rsk, Rku, Rmr(c)$	$R\Delta a, R\Delta q, peak curvature$	$R\lambda a, R\lambda q, Pc, correlation length$	none
Typical 3D parameters	$Sa, Sq$	$Ssk, Sku, Ssc$	$S\Delta a, Ssc$	$Sal, Sdr$	$Std, Svi$

Fig. 6 Effect of surface roughness and topography on sliding friction after Ref 3 with modifications. Key: double filled circle: much evidence

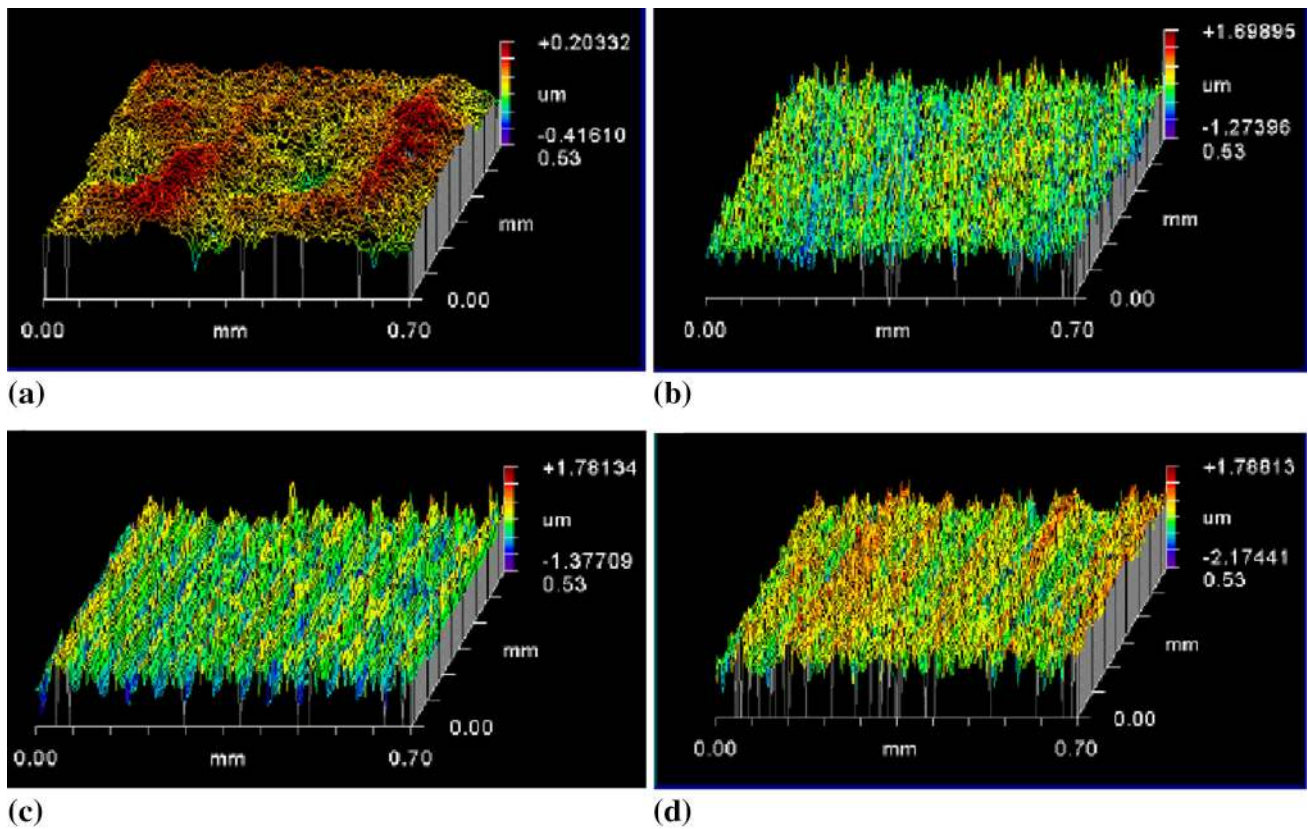


Fig. 7 Surface topographies produced by isotropic finishing (a), honing (b), hard turning (c) and grinding (d) (Ref 10)

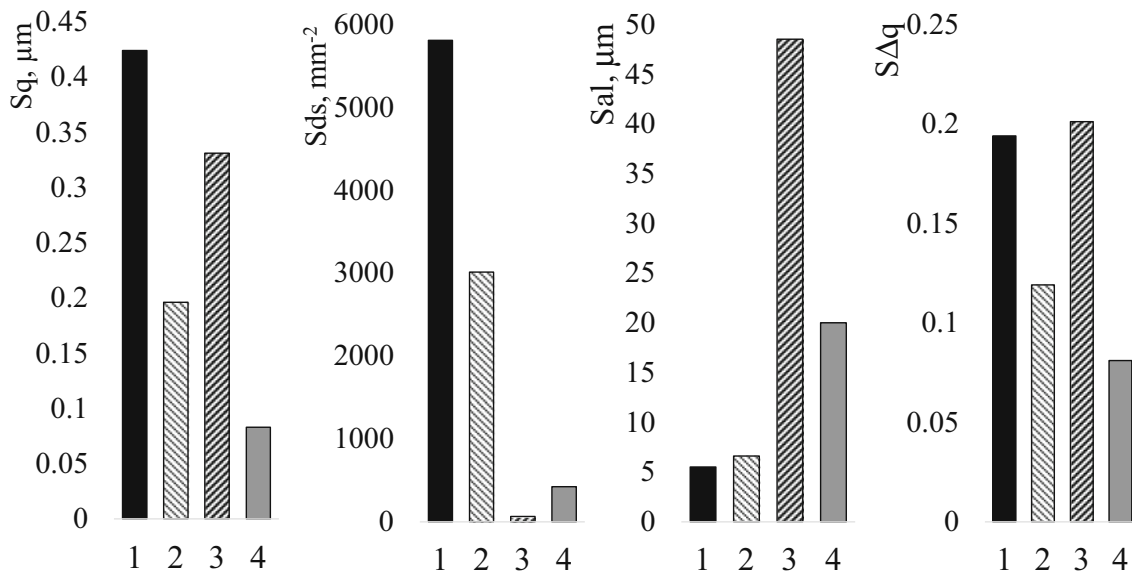
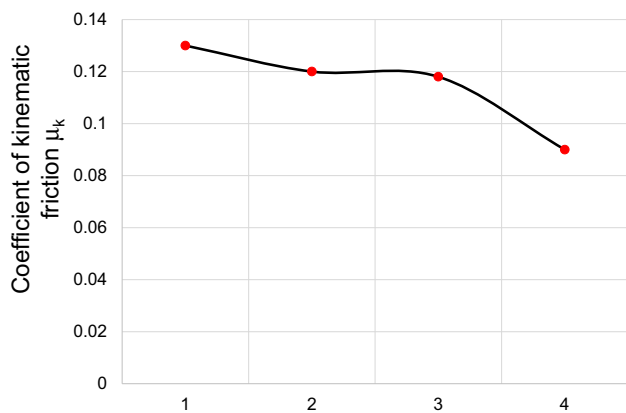


Fig. 8 Values of 3D roughness parameters for various finishing operations on hardened AISI 52100 bearing steel; 1-grinding, 2-hard turning, 3-honing, 4-isotropic finishing (data after Ref 9)

It was also found that for turned, milled and ground surfaces made of a 100Cr6 bearing steel, characterized by negative skewness, the friction is reduced when contacted surfaces are lubricated (Ref 13). Similar effect occurs when the reduced valley height  $Rvk$  is higher than the reduced peak height, i.e., when  $Rvk > Rpk$ .

#### 4. Abrasive Wear Resistance

Abrasive (tribological) wear of contacted surfaces depends distinctly on their structures independently of the type of friction conditions, i.e., dry or mixed with lubricant supply (Ref 4). The



**Fig. 9** Values of friction coefficient for various surface topographies produced on AISI 52100 bearing steel. 1-Ground, 2-honed, 3-hard turned, 4-isotropic finished ( $\mu_k$  values after Ref 11)

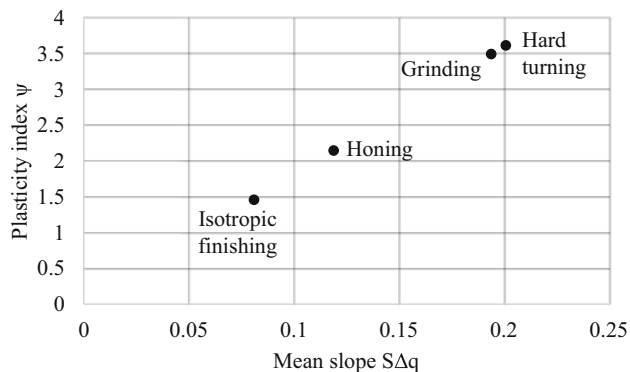


**Fig. 10** Dependence of plasticity index on the mean surface slope (values of  $\Psi$  and  $S\Delta q$  after Ref 11)

problem of the reduction of wear intensity of various tribo-pairs is very important at the design and technological levels.

Figure 11 presents the development of manufacturing processes of cylinder liners including traditional one-pass honing (a) producing net of crossing grooves inclined at 45 deg, *plateau* honing (b) producing oil pockets in the form of deeper grooves, helical honing (c) producing elongated grooves at 140 deg which ensure about 40% reduction of the wear in the reversal zone in comparison with *plateau* structure, laser texturing (d) which further reduces wear and friction losses and minimize the risk of seizure, and laser honing (e) producing deterministic structure of oil pockets which ensure 2-3 times smaller oil consumption and longer durability of the piston-rings system.

It should be added that the plateau surface of a cylinder liner is typically characterized according to ISO 13565-2 standard by five functional parameters—the reduced peak height  $R_{pk}$ , the core roughness depth  $R_k$ , the reduced valley depth  $R_{vk}$ , upper  $Mr_1$  and lower  $Mr_2$  material ratios, but ISO 13565-3 standard recommends also an  $R_q$  family more closely correlated with honing variables including the slope of the linear regression performed through the plateau region  $R_{pq}$ , the slope of linear regression for the valley region  $R_{vq}$ , and the intersection point of the normal probability graph of abscissa  $R_{mq}$  which defines the separation point of plateau and basic textures (Ref 1).

The groups of 2D and 3D surface roughness parameters which influence abrasive wear in sliding contact are specified in Fig. 12. It can be seen in Fig. 12 that the trends are the same as for sliding friction (Fig. 6).

Laser texturing as an effective way for reduction of abrasive wear is currently extended to such functional elements as piston rings, bearing raceways, brake and clutch plates (Fig. 13c). It should be noted that the main challenge for such tribological systems as brake and clutch plates is to intensify friction and increase the friction coefficient (Ref 4). It is reported (Ref 14) that friction coefficients as high as 1.6 were measured for the sliding interaction of specially designed textures. In addition, the reduction of the parasitic friction in operating machinery due to optimized surface texturing can be as much as 5% (Ref 15). In the case of surface topographies, their tribological properties were assessed based on their dependences on skewness  $S_{sk}$  and kurtosis  $S_{ku}$ . In summary, Fig. 12 depicts that wear as a very complex phenomenon depends on all groups of surface parameters including lays and leads (Ref 3).

New methods of characterizing and measuring both geometrical and physical properties of surface integrity produced by conventional cutting and abrasive machining operations are described in Ref 15 and 16.

Extended characterization of surface roughness and surface texture produced by different finishing processes on hardened steel parts is presented by Grzesik et al. for hard turned and ball burnished surfaces (Ref 17–19), and comparatively for hard turned, CBN ground, belt ground and superfinished surfaces (Ref 18, 20). Figures 14 and 15 show the comparison of the values of three functional (bearing) parameters—reduced core height ( $S_k$ ), reduced peak height ( $S_{pk}$ ) and reduced valley height ( $S_{vk}$ ), and corresponding three functional indexes—surface bearing index ( $S_{bi}$ ), core fluid retention index ( $S_{ci}$ ) and valley fluid retention index ( $S_{vi}$ ), respectively. Figure 14 shows that the minimum value of the reduced peak height  $S_{pk} = 0.09 \mu m$ , which corresponds to the minimum running-in period and minimum height of removed material, was obtained after superfinishing operation. On the other hand, the surface with the best tribological properties (lower wear of surface peaks), which correspond to the minimum value of the surface bearing index  $S_{bi} = 0.30$ , was generated by finish grinding using superhard CBN wheel. Moreover, the same surface indicates the best fluid retention ability, which corresponds to the maximum value of the valley fluid retention index  $S_{vi} = 0.14$ . In particular, hard turned surface with the highest value of the  $S_{ci}$  index equal to 1.71 should be predominantly applied when the better fluid retention ability within the core is required.

## 5. Adhesion and Bonding

In the case of adhesion and bonding, the most important parameter seems to be the developed surface area ratio  $S_{dr}$  expressed in % because the developed area of the joint surface is definitely more important than the  $S_a$  or  $S_z$  parameters. It should be noted that for an ideal flat surface  $S_{dr} = 0$ . As reported in Ref 21, two surfaces with practically the same value of  $S_a$  parameters can have about 200% higher value of  $S_{dr}$  parameter.

The groups of 2D and 3D surface roughness parameters which influence adhesion and bonding abilities in contact of rough surfaces are specified in Fig. 16.

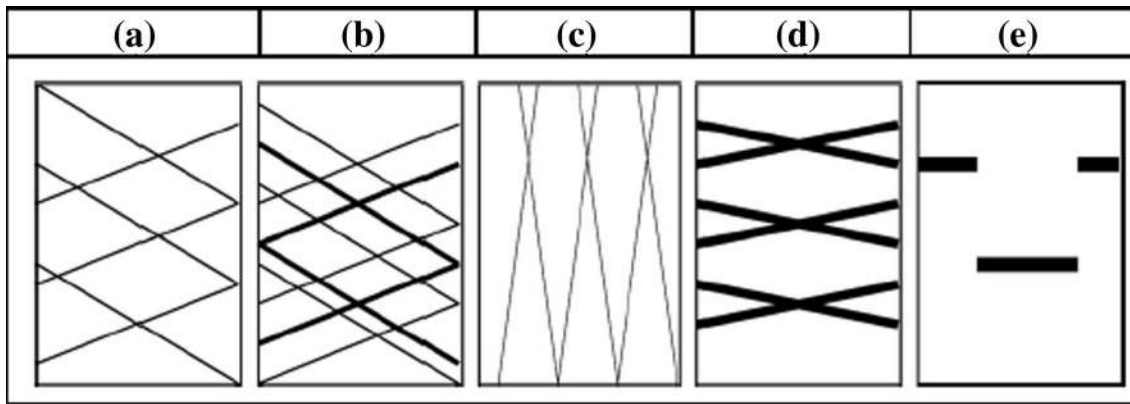


**Fig. 11** Possible modifications of surface topographies of cylinder liners in order to reduce engine oil consumption and running-in wear after Ref 1: one-pass honing (a), plateau honing (b), helical honing (c), laser honing (texturing) (d), regular structure of oil pockets (e)

Function \ Surface parameters	Height	Amplitude and shape	Hybrid and curvature	Length and peak space	Lays and texture
<b>Wear</b>	● ●	● ●	● ●	● ●	● ●
Typical 2D parameters	$Ra, Rq, Rt$	$Rsk, Rku, Rmr(c)$	$R\Delta a, R\Delta q, \text{peak curvature}$	$R\lambda a, R\lambda q, Pc, \text{correlation length}$	<i>none</i>
Typical 3D parameters	$Sa, Sq$	$Ssk, Sku, Ssc$	$S\Delta a, Ssc$	$Sal, Sdr$	$Std, Svi$

**Fig. 12** Effect of surface finish and topography on wear after Ref 3 with modifications. Key: double filled circle: much evidence

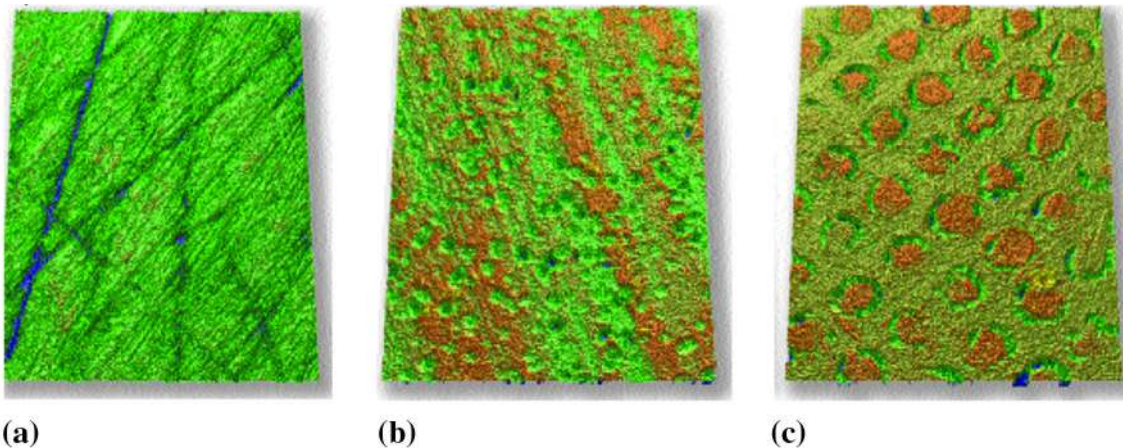


**Fig. 13** Surfaces of clutch plates with various topographies after Ref 14: (a) crossing lays, (b) micro-finished, (c) textured with regular pits

It is evident based on engineering practice and also simple engineering logic that the machined surface with a larger developed area ensures more strong adhesive joint with another surface. As a result, the deposited coating adheres stronger to the substrate. On the other hand, the area of developed surface depends on the height and amplitude surface parameters including  $Sq, Ssk, Sku$  and  $Ssc$  parameters (see Fig. 16).

## 6. Corrosion Resistance

In general, higher surface roughness weakens corrosion resistance due to the fact that the real contact area increases (Ref 4). As a result, the corrosion wear is decisively influenced by height roughness parameters (predominantly  $Sz$  parameter) and the arithmetic mean summit curvature  $Ssc$ . The negative

role of strain-hardening effect is also reported because peaks are more deformed than grooves.

It can be seen in Fig. 17 that the surface textures more exposed to corrosion have distinctly deeper valleys (surface (b) in Fig. 17). In contrast, surfaces more resistant to corrosion are more anisotropic (surface (a) in Fig. 17). In the second case, a

surface with a Gaussian height distribution ( $S_{sk} = 0$ ,  $S_{ku} = 3$ ) is selected (Ref 4).

Corrosion resistance can also be related to the shape of bearing area curve (BAC) and especially corresponds with the valley fluid retention index  $S_{vi}$ . Surfaces with a linear bearing area curve indicate higher resistance to corrosion than degressive-progressive types of BAC's with negative skewness  $S_{sk} < 0$ . In addition, lays play an important role in the stress corrosion, as for instance for milled surfaces (Ref 23).

## 7. Summary

This paper presents the state-of-the-art the knowledge concerning the relationships between surface roughness/surface texture and fundamental functional properties such as fatigue, tribological behavior, corrosion resistance and adhesion and bonding strength.

Although this knowledge is not complete, some strong correlations between functional properties and measured 2D/3D surface roughness parameters are established. In general, these correlations are not based on one predominant roughness parameter but depend on several groups of roughness parameters including surface texture and its specific characteristics as for instance the texture aspect ratio  $Str$  or the texture direction  $Std$ .

Moreover, in the light of the survey performed, the use of only one or a group of height roughness parameters— $R_a$  or  $R_a$ ,  $R_q$ ,  $R_z$ ,  $R_t$ —is highly insufficient. For instance, prediction of

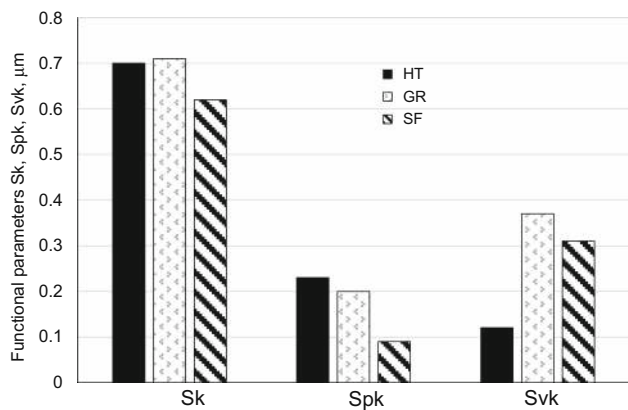


**Fig. 14** Influence of finishing process on values of functional surface parameters  $S_k$ ,  $S_{pk}$  and  $S_{vk}$

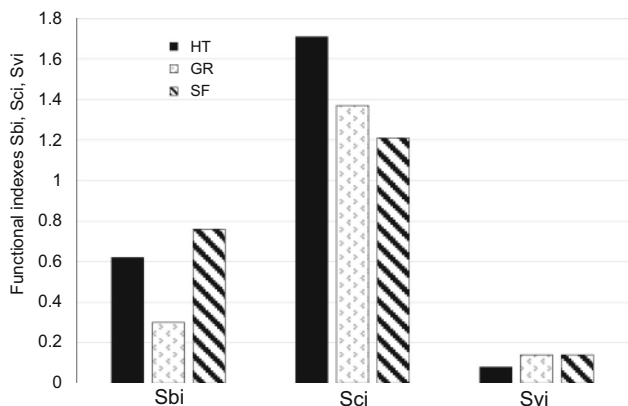


**Fig. 15** Influence of finishing process on values of functional indexes  $S_{bi}$ ,  $S_{ci}$  and  $S_{vi}$

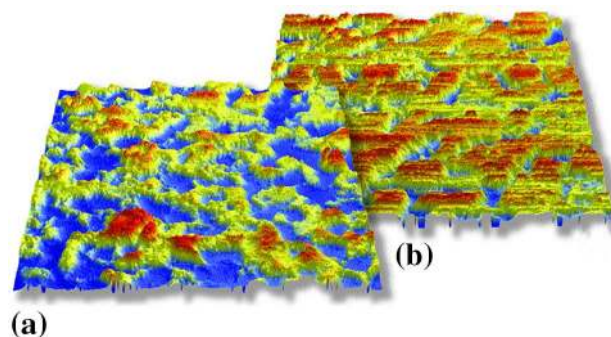


**Fig. 17** Comparison of surface topographies which does not tend (a) and tend (b) to rust after Ref 22

Function \ Surface parameters	Height	Amplitude and shape	Hybrid and curvature	Length and peak space	Lays and texture
<b>Adhesion and bonding</b>	● ●	● ●	●	●	●
Typical 2D parameters	$R_a$ , $R_q$ , $R_t$	$R_{sk}$ , $R_{ku}$ , $R_{mr}(c)$	$R_{\Delta a}$ , $R_{\Delta q}$ , peak curvature	$R_{\lambda a}$ , $R_{\lambda q}$ , $P_c$ , correlation length	none
Typical 3D parameters	$S_a$ , $S_q$	$S_{sk}$ , $S_{ku}$ , $S_{sc}$	$S_{\Delta a}$ , $S_{sc}$	$S_{al}$ , $S_{dr}$	$S_{td}$ , $S_{vi}$

**Fig. 16** Effect of surface finish and topography on adhesion and bonding after Ref 3 with modifications. Key: double filled circle: much evidence



fatigue life required more parameters including the amplitude and hybrid parameters (Rsk, Rku, Rdq) as well as 3D surface texture parameters (Str, Std, Sal).

Tribological properties and fluid retention ability can be characterized using both functional height parameters (Spk, Sk, Svk) and functional indexes related to peak zone, core material and valley zone (Sbi, Sci, Svk).

Final conclusion is that R&D centers should be deeply engaged in the problems concerning the functional performance of machined parts with demanded functional properties and its correlations with surface finish and in a broader sense with surface integrity (Ref 15, 16).

## Open Access

This article is distributed under the terms of the Creative Commons Attribution 4.0 International License (<http://creativecommons.org/licenses/by/4.0/>), which permits unrestricted use, distribution, and reproduction in any medium, provided you give appropriate credit to the original author(s) and the source, provide a link to the Creative Commons license, and indicate if changes were made.

## References

1. T.G. Mathia, P. Pawlus, and M. Wiczorowski, Recent Trends in Surface Metrology, *Wear*, 2011, **271**(3-4), p 494–508
2. X.J. Jiang and D.V. Whitehouse, Technological Shifts in Surface Metrology, *CIRP Manuf. Technol.*, 2012, **61**(2), p 815–836
3. B. Griffiths, *Manufacturing Surface Technology*, Penton Press, London, 2001
4. T. Burakowski, *Areology. Theoretical Fundamentals*, Institute of Exploitation Technology, Radom, 2013 (in Polish)
5. D.J. Whitehouse, Function Maps and the Role of Surfaces, *Int. J. Mach. Tools Manuf.*, 2001, **41**(13-14), p 1847–1861
6. R. Leach, Ed., *Characterization of Areal Surface Texture*, Springer, Berlin, 2013
7. K.J. Stout and L. Blunt, *Three Dimensional Surface Topography*, Penton Press, London, 2000
8. D. Novocic, R.C. Dewes, D.K. Aspinwall, W. Voice, and P. Bowen, The Effect of Machined Topography and Integrity on Fatigue Life, *Int. J. Mach. Tools Manuf.*, 2004, **44**(2-3), p 125–134
9. K.J. Kubiak, T.W. Liskiewicz, and T.G. Mathia, Surface Morphology in Engineering Applications: Influence of Roughness on Sliding and Wear in Dry Fretting, *Tribol. Int.*, 2011, **44**(11), p 1427–1432
10. R. Sing, S.N. Melkote, and F. Hashimoto, Frictional Response of Precision Finished Surfaces in Pure Sliding, *Wear*, 2005, **258**(10), p 1500–1509
11. F. Hashimoto, S.N. Melkote, R. Singh, R. Kalil, Effect of Finishing Methods on Surface Characteristics and Performance of Precision Components in Rolling/Sliding Contact, in *Proceedings of 10th International Workshop on Modeling of Machining Operations*, Sintra, 2010, p. 21
12. N. Tayebi and A.A. Polycarpou, Modeling the Effect of Skewness and Kurtosis on the Static Coefficient of Rough Surfaces, *Tribol. Int.*, 2004, **37**(6), p 491–505
13. M. Sedlacek, B. Podgornik, and J. Vizitin, Influence of Surface Preparation on Roughness Parameters, Friction and Wear, *Wear*, 2009, **266**(3-4), p 482–487
14. A.A.G. Bruzzone, H.L. Costa, P.M. Lonardo, and D.A. Lucca, Advances in Engineered Surfaces for Functional Performance, *CIRP Manuf. Technol.*, 2008, **57**(2), p 750–769
15. I.S. Jawahir, E. Brinksmeier, R. M'Saoubi et al., Surface Integrity in Removal Processes: Recent adVances, *CIRP Ann. Manuf. Technol.*, 2012, **60**(2), p 603–626
16. W. Grzesik, Chapter 20-Surface Integrity, in *Advanced Machining Processes of Metallic Materials* (Elsevier, Amsterdam, 2008), pp. 405–426
17. W. Grzesik and K. Zak, Producing High Quality Hardened Parts Using Sequential Hard Turning and Ball Burnishing Operations, *Precis. Eng.*, 2013, **37**, p 849–855
18. W. Grzesik, J. Rech, and K. Zak, Characterization of Surface Textures Generated on Hardened Steel Parts in High-Precision Machining Operations, *Int. J. Adv. Manuf. Technol.*, 2015, **78**, p 2049–2056
19. W. Grzesik and K. Zak, Characterization of Surface Integrity Produced by Sequential Dry Hard Turning and Ball Burnishing Operations, *J. Manuf. Sci. Eng.*, 2014, **136**, p 031017-1–031017-9
20. W. Grzesik, J. Rech, and T. Wanat, Surface Finish on Hardened Bearing Steel Parts Produced by Superhard and Abrasive Tools, *Int. J. Mach. Tools Manuf.*, 2007, **47**, p 255–262
21. G. Stachowiak and P. Podsiadlo, 3-D Characterization, Optimization, and Classification of Textured Surfaces, *Tribol. Lett.*, 2008, **32**(1), p 13–21
22. M. Zecchino, Characterizing Surface Quality: Why Average Roughness is Not Enough (2003). [www.veeco.com](http://www.veeco.com)
23. K.L. Lyon, T.J. Marrow, and S.B. Lyon, Influence of Milling on the Development of Stress Corrosion Cracks in Austenitic Stainless Steel, *J. Mater. Process. Technol.*, 2015, **218**, p 32–37